Transp Porous Med (2010) 85:157–169
DOI 10.1007/s11242-010-9552-5

Generalized Plain Couette Flow and Heat Transfer in a Composite Channel

J. C. Umavathi · Ali J. Chamkha · K. S. R. Sridhar

Received: 14 March 2009 / Accepted: 17 February 2010 / Published online: 6 March 2010

Abstract An analytical study of fluid flow and heat transfer in a composite channel is presented. The channel walls are maintained at different constant temperatures in such a way that the temperatures do not allow for free convection. The upper plate is considered to be moving and the lower plate is fixed. The flow is modeled using Darcy–Lapwood–Brinkman equation. The viscous and Darcy dissipation terms are included in the energy equation. By applying suitable matching and boundary conditions, an exact solution has been obtained for the velocity and temperature distributions in the two regions of the composite channel. The effects of various parameters such as the porous medium parameter, viscosity ratio, height ratio, conductivity ratio, Eckert number, and Prandtl number on the velocity and temperature fields are presented graphically and discussed.

Keywords Porous media · Couette flow · Composite channel · Analytical solution

List of Symbols

C_p Specific heat at constant pressure
Ec Eckert number $\left(\frac{U^2}{C_p(T_{w1}-T_{w2})}\right)$
h Ratio of the heights of the two regions $\left(\frac{h_2}{h_1}\right)$
h_i Height of the channel
p Pressure

J. C. Umavathi
Department of Mathematics, Gulbarga University, Gulbarga 585 106, Karnataka, India

A. J. Chamkha (✉)
Manufacturing Engineering Department, The Public Authority for Applied Education and Training, Shuweikh 70654, Kuwait
e-mail: achamkha@yahoo.com

K. S. R. Sridhar
Department of Mathematics, Bellary Engineering College, Bellary 583 104, Karnataka, India

P	Non-dimensional pressure gradient $\left(\frac{h_1^2}{\mu_1 U}\frac{dp}{dx}\right)$
Pr	Prandtl number $\left(\frac{\mu_1 C_p}{\psi_1}\right)$
U	Velocity of the upper plate
u_i	Velocity
T_i	Temperature
T_{w}	Wall temperature
x, y	Space coordinates

Greek Symbols

κ	Permeability of the porous medium
σ	Porous medium parameter $\left(\frac{h_1}{\sqrt{\kappa}}\right)$
ψ_i	Thermal conductivity
μ_i	Viscosity
λ	Viscosity ratio $\left(\frac{\mu_2}{\mu_1}\right)$
λ_T	Conductivity ratio $\left(\frac{\psi_2}{\psi_1}\right)$
ΔT	Difference in temperature $(T_{w1} - T_{w2})$
θ_i	Non-dimensional temperature $\left(\frac{T_i - T_{w2}}{T_{w1} - T_{w2}}\right)$

Subscript

$i = 1, 2$ Quantities for regions I and II, respectively

1 Introduction

The investigation of forced convection flows in saturated porous media is required in many thermal engineering applications. Several numerical and experimental studies have been conducted in order to provide a deeper understanding of the transport mechanism of momentum and heat transfer in porous media. Porous media have a wide range of applications such as catalytic and inert bed reactors, enhancing drying efficiency such as food drying, filtering, geothermal energy management and harvesting, insulation, lubrication (Kaviany 1995), ground water and oil flow, and enhancing oil and natural gas production.

A composite layer comprising a fluid layer adjacent to a layer of fluid-saturated porous medium is of common occurrence in many a situation present in the aforementioned application areas. Composite systems are part of numerous other engineering applications also, such as fibrous and granular insulation, porous insulation of ducts, ambient air heat transfer from hair covered skin, grain storage, and drying paper. Freezing of soils and melting of ice frozen soils due to the change in weather conditions also require the knowledge of interaction mechanism between the fluid and porous layers. Composite layers also find application in porous journal bearings.

Recently, heat transfer in channels partially filled with porous media has received considerable attention and was the focus of several investigations (Chikh et al. 1995 and Vafai and Kim 1990). As previously mentioned, the need for better understanding of heat transfer in

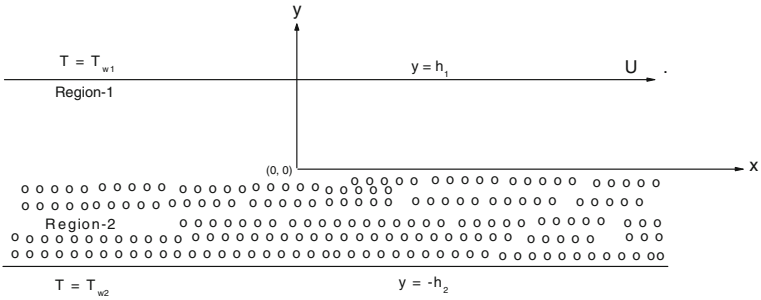

Fig. 1 Physical configuration

porous media is motivated by numerous engineering applications encountered. In general, most analytical studies of fluid flow adopt Darcy's law. In the study conducted by Al-Nimr and Alkam (1998), there appears to be very limited research on the problem of forced convection in composite fluids and porous layers. Beavers and Joseph (1967) first investigated the fluid mechanics at the interface between fluid layer and a porous medium over a flat plate. Rudraiah (1985) investigated the same problem using Darcy–Brinkman model. Neild (1991) discussed the limitation of the Brinkman–Forchheimer model in porous media and at the interface, between the clear fluid and porous region. Later on Vafai and Kim (1995) presented an exact solution for the same problem.

Composite layer flows are exciting because of the modeling challenge that is thrown at researchers to model interface and boundary condition/s. By browsing the literature, it becomes evident that the interface conditions which have been in use are either of the 'slip' or 'stick' type of condition (see Beavers and Joseph 1967 and Ochoa-Tapia and Whitaker 1995). Several works have appeared on composite layer flows using these conditions or variant of them (Vafai and Kim 1990; Kuznetsov 1998; Alazami and Vafai 2001; Umavathi et al. 2001, 2007 and the references therein).

Based on our review of the current literature, it is evident that very few studies are available on flow and heat transfer for generalized Couette flow. Thus, it is the objective of this study to investigate the effects of porous medium parameter and viscous forces on composite porous layers in the horizontal channel.

2 Mathematical Model

The physical configuration (Fig. 1) consists of a composite layer between two infinite parallel plates maintained at different constant temperatures, extending in the z and x directions. The region $0 \leq y \leq h_1$ (Region-I) is filled with a clear viscous fluid having viscosity μ_1 and thermal conductivity ψ_1. The region $-h_2 \leq y \leq 0$ (Region-II) is filled with homogeneous isotropic porous material having permeability κ. This region is saturated with a viscous fluid having viscosityμ_2 and thermal conductivity ψ_2. It is assumed that the flow is steady, laminar, fully developed, and that fluid properties are constant. The flow in both regions is assumed to be driven by a common constant pressure gradient $\left(-\frac{\partial p}{\partial x}\right)$ and temperature gradient $\Delta T = (T_{\mathrm{w1}} - T_{\mathrm{w2}})$where T_{w1} is the temperature of the boundary at $y = h_1$ and T_{w2} at $y = -h_2$. The upper plate is moving with a velocity U.

The Darcy model, which assumes proportionality between the velocity and pressure gradient, has been extensively used to investigate a number of interesting fluid and heat transfer problems associated with heated bodies embedded in fluid-saturated porous media. The model, however, is valid only for slow flows through porous media with low permeability (see Nakayama et al. 1990). At higher flow rates or in highly porous media there is a departure from the linear law and inertial effects become important. Most of the theoretical work has been based on Darcy's law, and as noted by Prasad et al. (1985), the experimental results never agreed with the theoretical results obtained with Darcy model. This has led to the inclusion of inertia and viscous effects in studies of convection in porous media (Prasad 1990). As a first step toward introducing this complexity into the problem, we consider only the Brinkman extended Darcy model to obtain realistic prediction. It is also assumed that at any given instant, the temperature of the fluid and temperature of the solid are same.

Under these assumptions, the governing equations of motion and energy for incompressible fluids are (Nield and Bejan 1999)

Region-I

$$\mu_1 \frac{\mathrm{d}^2 u_1}{\mathrm{d}y_1^2} = \frac{\mathrm{d}p}{\mathrm{d}x} \tag{1}$$

$$\psi_1 \frac{\mathrm{d}^2 T_1}{\mathrm{d}y_1^2} + \mu_1 \left(\frac{\mathrm{d}u_1}{\mathrm{d}y_1}\right)^2 = 0 \tag{2}$$

Region-II

$$\mu_2 \frac{\mathrm{d}^2 u_2}{\mathrm{d}y_2^2} - \frac{\mu_2}{\kappa} u_2 = \frac{\mathrm{d}p}{\mathrm{d}x} \tag{3}$$

$$\psi_2 \frac{\mathrm{d}^2 T_2}{\mathrm{d}y_2^2} + \mu_2 \left(\frac{\mathrm{d}u_2}{\mathrm{d}y_2}\right)^2 + \frac{\mu_2}{\kappa} u_2^2 = 0 \tag{4}$$

where u_i is the x-component of fluid velocity and T_i is the fluid temperature. The subscripts 1 and 2 denote the values for Region-I and Region-II, respectively. The direct numerical simulation (Martys et al. 1994) and experimental investigation (Giveler and Altobelli 1994) have demonstrated that there are situations when it is important to distinguish between effective viscosity and fluid viscosity. For example, in Giveler and Altobelli (1994) a water flow through a tube filled with an open-cell rigid foam of high porosity was investigated. It was obtained that for this flow $\mu_{\text{eff}} = \left(7.5^{+3.4}_{-2.4}\right)\mu_f$. However, most works used the Brinkman model assuming that the fluid viscosity and the Brinkman viscosity (i.e., effective viscosity) are same. In this model it is assumed that fluid viscosity and the Brinkman viscosity are same. The boundary conditions on velocity are no-slip conditions requiring that the velocity must vanish at the wall. The boundary conditions on temperature are isothermal conditions. The two boundaries are held at constant different temperatures. In addition, the continuity of velocity, shear stress, temperature, and heat flux at the interface between the porous and fluid layer are assumed.

The boundary and interface conditions on velocity and temperature are

$$\begin{aligned} &u_1(h_1) = U && T_1(h_1) = T_{w1} \\ &u_2(-h_2) = 0 && T_2(h_2) = T_{w2} \\ &u_1(0) = u_2(0) && T_1(0) = T_2(0) \\ &\mu_1 \frac{du_1}{dy} = \mu_2 \frac{du_2}{dy} \text{ at } y = 0 && \psi_1 \frac{dT_1}{dy} = \psi_2 \frac{dT_2}{dy} \text{ at } y = 0 \end{aligned} \tag{5}$$

Equations 1–4 along with boundary and interface conditions (5) are made dimensionless by using the following transformations.

$$u_1^* = \frac{u_1}{U}; u_2^* = \frac{u_2}{U}; y_1^* = \frac{y_1}{h_1}; y_2^* = \frac{y_2}{h_2}; \theta = \frac{T - T_{w2}}{T_{w1} - T_{w2}}; P = \frac{h_1^2}{\mu_1 U}\frac{dp}{dx}$$
$$\sigma = \frac{h_1}{\sqrt{\kappa}}; \text{Ec} = \frac{U^2}{C_p(T_{w1} - T_{w2})}; \text{Pr} = \frac{\mu_1 C_p}{\psi_1}; \lambda = \frac{\mu_2}{\mu_1}; \lambda_T = \frac{\psi_2}{\psi_1}; h = \frac{h_2}{h_1}. \tag{6}$$

The non-dimensional governing equations become

Region-I

$$\frac{d^2u_1}{dy_1^2} = P \tag{7}$$

$$\frac{d^2\theta_1}{dy_1^2} + Ec\,\text{Pr}\left(\frac{du_1}{dy_1}\right)^2 = 0 \tag{8}$$

Region-II

$$\frac{d^2u_2}{dy_2^2} - \sigma^2 h^2 u_2 = \frac{h^2}{\lambda} P \tag{9}$$

$$\frac{d^2\theta_2}{dy_2^2} + \frac{Ec\,\text{Pr}\,\lambda}{\lambda_T}\left(\frac{du_2}{dy_2}\right)^2 + \frac{Ec\,\text{Pr}\,\lambda\sigma^2 h^2}{\lambda_T} u_2^2 = 0 \tag{10}$$

The non-dimensional form of the velocity, temperature boundary, and interface conditions are

$$\begin{aligned} &u_1(1) = 1 && \theta_1(1) = 1 \\ &u_2(-1) = 0 && \theta_2(-1) = 0 \\ &u_1(0) = u_2(0) && \theta_1(0) = \theta_2(0) \\ &\frac{du_1}{dy} = \frac{\lambda}{h}\frac{du_2}{dy} \text{ at } y = 0 && \frac{d\theta_1}{dy} = \frac{\lambda_T}{h}\frac{d\theta_2}{dy} \text{ at } y = 0 \end{aligned} \tag{11}$$

The asterisks have been dropped for simplicity.

3 Solutions

The momentum and energy Eqs. 7–10 are solved subject to the boundary and interface conditions (11) for the velocity and temperature distributions. The basic equations are linear ordinary differential equations and hence closed-form solutions are obtained. Equations 7 and 9 are solved for the velocity field in Region-I and Region-II. The integrating constants

c_1, c_2 obtained from Eq. 7 and c_3, c_4 obtained from Eq. 9 are solved simultaneously using boundary and interface conditions as defined in Eq. 11. Using these solutions, energy Eqs. 8 and 10 are integrated twice to obtain temperature fields. The integrating constants k_1, k_2 of Eq. 8 and k_3, k_4 of Eq. 10 are evaluated simultaneously using boundary and interface conditions as defined in Eq. 11. The solutions are given below.

$$u_1 = \frac{Py_1^2}{2} + c_1 y_1 + c_2 \tag{12}$$

$$u_2 = c_3 C\ \mathrm{osh}\,(\sigma h y_2) + c_4 S\ \mathrm{inh}\,(\sigma h y_2) - \frac{Ph^2}{\lambda\sigma^2} \tag{13}$$

$$\theta_1 = b_1 y_1^4 + b_2 y_1^3 + b_3 y_1^2 + k_1 y_1 + k_2 \tag{14}$$

$$\theta_2 = f_1 C\ \mathrm{osh}\,(2\sigma h y_2) + f_2 S\ \mathrm{inh}\,(2\sigma h y_2) + f_3 S\ \mathrm{inh}\,(\sigma h y_2) + f_4 Cosh\,(\sigma h y_2) + f_5 y_2^2 + k_3 y_2 + k_4 \tag{15}$$

where the expressions for the constants appearing in the solutions are given in the Appendix.

Apart from the velocity and temperature distributions in the channel, it is important to determine the heat flux between the plates and fluid. The heat flux through the channel wall to the fluid is given by

$$q = \psi \left(\frac{\partial T}{\partial y}\right)_{y=h_1,-h_2} \tag{16}$$

A measure of the effectiveness of heat transfer is provided by the Nusselt number which is defined as

$$\mathrm{Nu} = \frac{(\text{heat flux})\ (\text{height of the channel})}{\psi\,(\text{temperature difference})}$$

The Nusselt numbers at the top and bottom walls are given, respectively, by

$$\mathrm{Nu}_+ = (1+h)\left(\frac{\mathrm{d}\theta}{\mathrm{d}y}\right)_{y=1} \tag{17}$$

$$\mathrm{Nu}_- = \left(1+h^{-1}\right)\left(\frac{\mathrm{d}\theta}{\mathrm{d}y}\right)_{y=-1} \tag{18}$$

4 Results and Discussion

Exact solutions for flow and heat transfer for Couette flow containing fluid and porous layer are obtained and reported in the previous section. These solutions are evaluated numerically and depicted graphically in Figs. 2, 3, 4, 5, 6, 7, 8, 9 and 10.

The variations of velocity and temperature for different values of porous medium parameter σ are shown in Figs. 2 and 5, respectively. For large porous medium parameter σ, the frictional drag resistance against the conduction is very large and as a result, the velocity and temperature are very small in porous region. As the porous medium parameter σ decreases, the fluid velocity and temperature increase significantly.

The effects of the viscosity ratio λ on the velocity and temperature are shown in Figs. 3 and 6, respectively. As the ratio of viscosities of fluid in porous medium and fluid in clear region increases, both the velocity and temperature profiles decrease. It is seen from Fig. 3 that for $\lambda = 0.5$ i.e., viscosity of the clear fluid is twice the viscosity of the porous medium, but still the velocity is more for clear fluid.

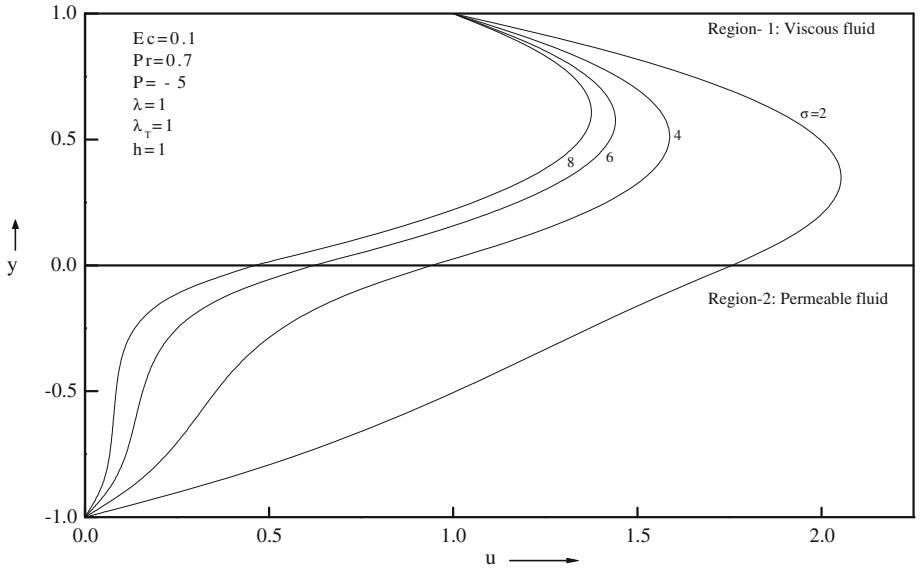

Fig. 2 Velocity profiles for different values of porous parameter σ

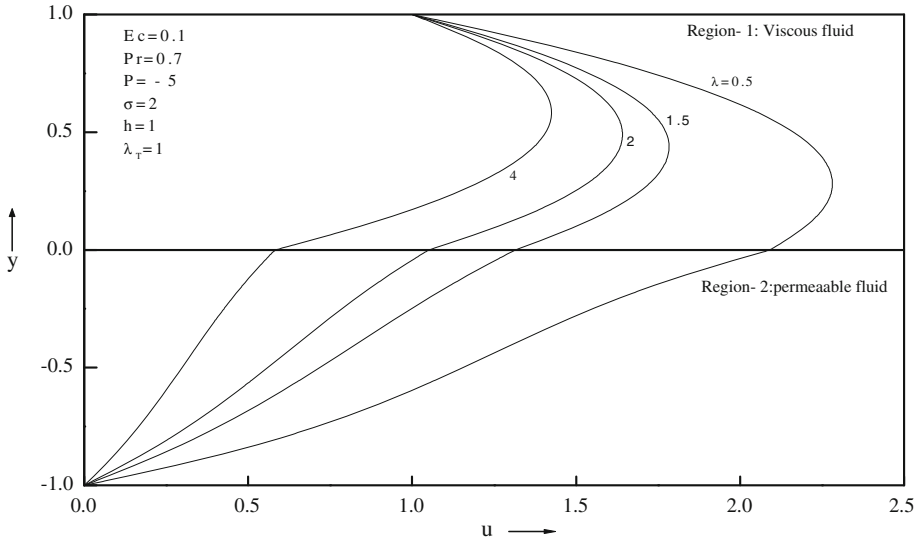

Fig. 3 Velocity profiles for different values of viscosity ratio λ

The effects of the height ratio h on the velocity and temperature fields are depicted in Figs. 4 and 7, respectively. As the height ratio h increases, the velocity profile decreases while the temperature profile increases. That is, the larger the height of the permeable fluid, the lower the velocity field and the higher the temperature field. We observe from this figure that the ratio of heights has a significant effect on the flow.

The effect of the conductivity ratio λ_T on the temperature is shown in Fig. 8. As the conductivity ratio λ_T increases, the temperature decreases at any given point. That is, the

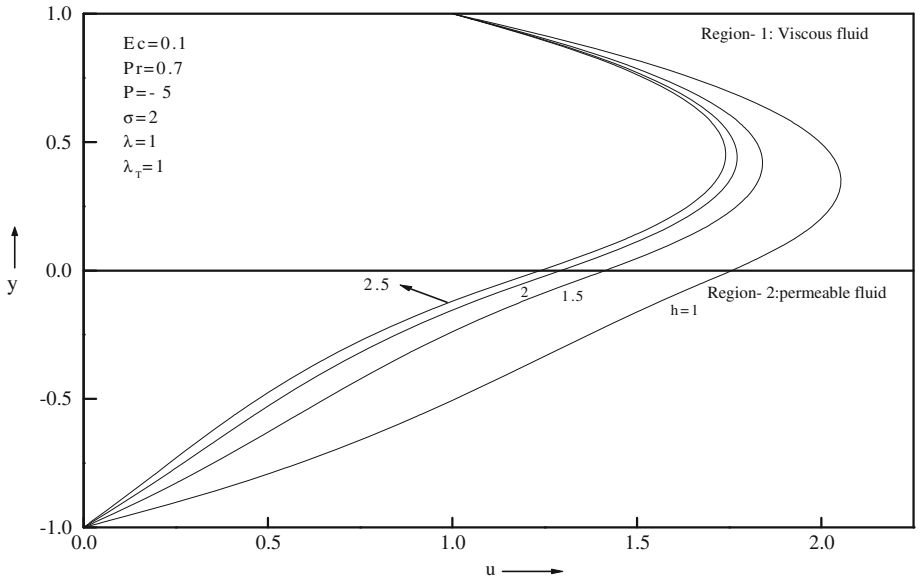

Fig. 4 Velocity profiles for different values of width ratio h

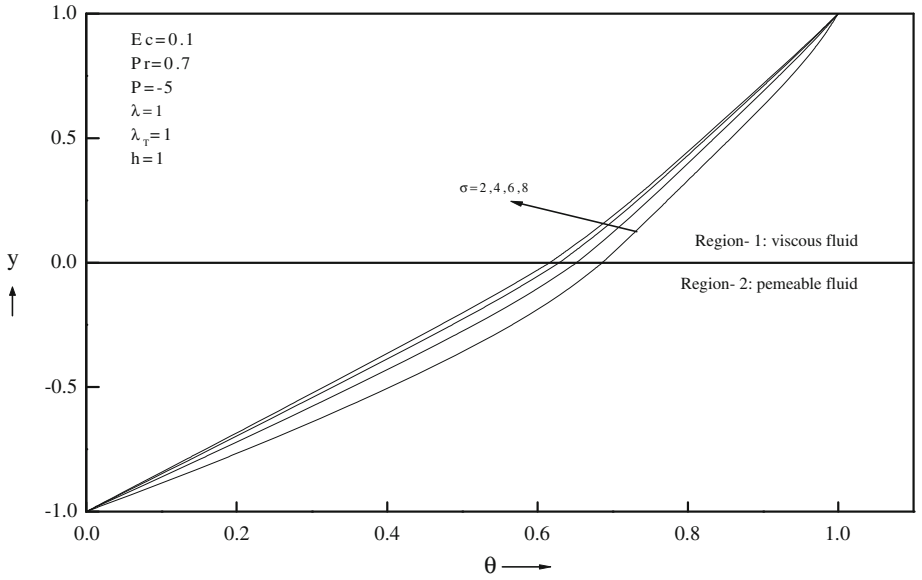

Fig. 5 Temperature profiles for different values of porous parameter σ

larger the conductivity of the permeable fluid compared to the viscous fluid, the smaller the amount of heat transfer.

The effects of the Eckert number Ec and the Prandtl number Pr on the temperature are shown in Figs. 9 and 10, respectively. The temperature increases as either of the Eckert

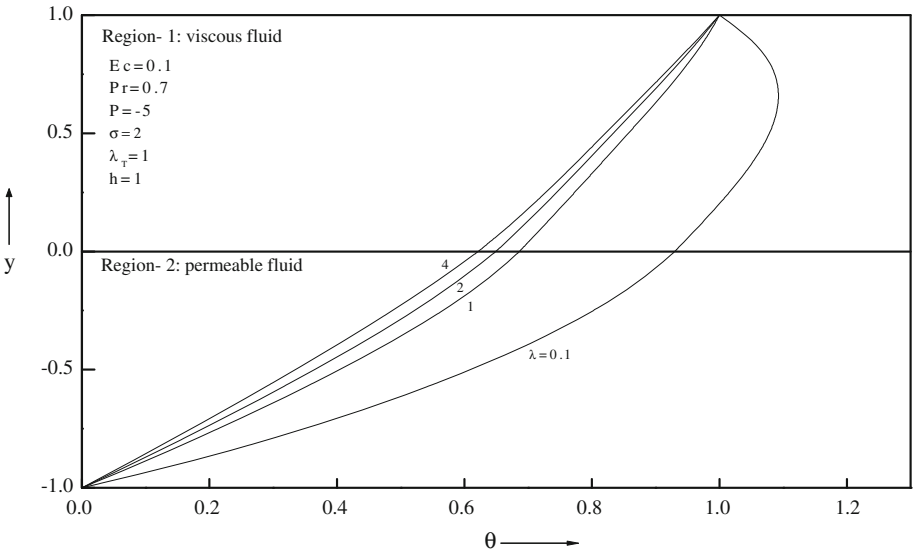

Fig. 6 Temperature profiles for different values of viscosity ratio λ

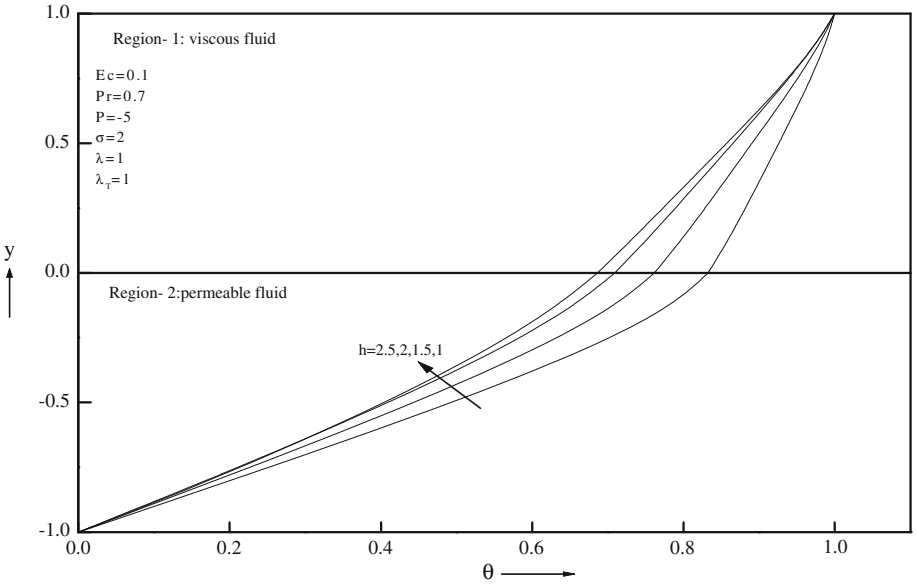

Fig. 7 Temperature profiles for different values of width ratio h

number or the Prandtl number increases. This is an expected result as seen from the energy equation.

The variation of the Nusselt number with different physical parameters fixing the other parameters is given in Table 1. We observe that as the height ratio increases, the Nusselt number at the upper plate decreases whereas it increases at the lower plate. The effect of the conductivity ratio and the porous medium parameter is to increase the Nusselt number at the

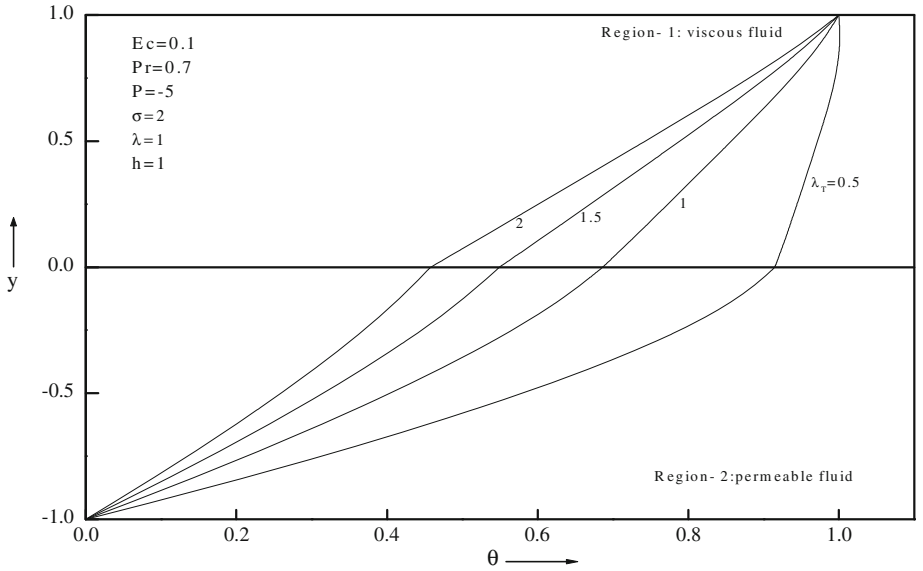

Fig. 8 Temperature profiles for different values of conductivity ratio λ_T

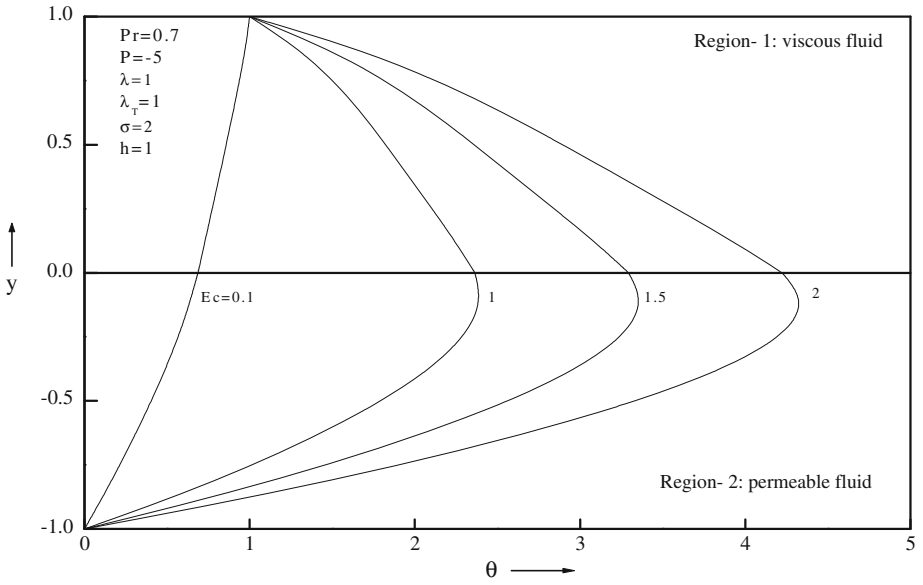

Fig. 9 Temperature profiles for different values of Eckert number *Ec*

top plate and decrease at the bottom plate. The effect of the Eckert number and the Prandtl number is to decrease the Nusselt number at the top plate and increase at the bottom plate. The effect of viscosity ratio is to suppress the Nusselt number at both the top and bottom plates. The values of h, λ_T, Ec, λ, Pr and σ are varied from 0.5 to 2.5 as shown in Table 1.

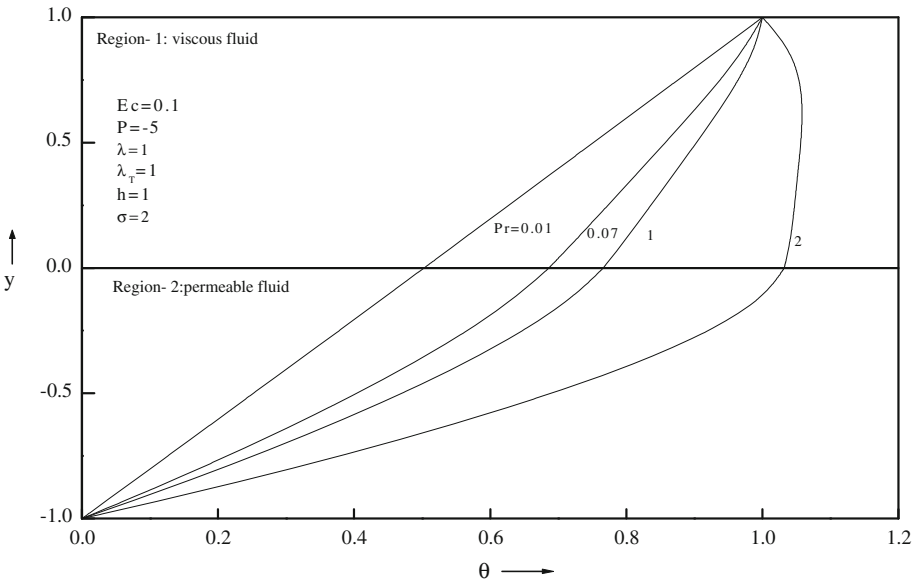

Fig. 10 Temperature profiles for different values of Prandtl number Pr

Table 1 The variation of the Nusselt number with different physical parameters for $\sigma = 2, h = 1, \lambda = 1, \lambda_T = 1, Ec = 0.1, \Pr = 0.7$

h	Nu_+	Nu_-	λ_T	Nu_+	Nu_-	Ec	Nu_+	Nu_-
0.5	0.7924	1.3139	0.5	−0.1043	2.7470	0.5	−2.2343	5.1549
1.0	0.3531	1.8309	1.0	0.3531	1.8309	1.0	−5.4687	9.3099
1.5	−1.9100	5.2158	1.5	0.6276	1.4036	1.5	−8.7031	13.464
2.0	−12.202	20.442	2.0	0.8106	1.1442	2.0	−11.937	17.619
2.5	−47.293	70.114	2.5	0.9413	0.9676	2.5	−15.171	21.774
h	Nu_+	Nu_-	Pr	Nu_+	Nu_-	θ	Nu_+	Nu_-
0.5	1.0172	2.1231	0.5	0.5379	1.5935	0.5	0.0688	2.3648
1.0	0.3531	1.8309	1.0	0.0758	2.1871	1.0	0.1585	2.1956
1.5	0.4838	1.6808	1.5	−0.3861	2.7807	1.5	0.2616	2.0020
2.0	0.5504	1.5865	2.0	−0.8482	3.3742	2.0	0.3531	1.8309
2.5	0.5901	1.5215	2.5	−1.3102	3.9678	2.5	0.4260	1.6957

5 Conclusions

Couette flow and heat transfer for composite porous layer was investigated analytically. Closed-form solutions were obtained for the governing equations of the flow and thermal problems and were shown graphically. In addition, results for the rate of heat transfer for different values of the physical parameters were presented in tabular form. It was found that the effects of the porous medium parameter and viscosity ratio suppressed the velocity, and height ratio promotes the velocity. The effects of the porous medium parameter and the viscosity ratio were found to decrease the temperature field whereas the height ratio, Prandtl number, and the Eckert number promoted the temperature. The rate of the heat transfer was promoted at the top plate by increasing the conductivity ratio and the porous medium

parameter but it decreased with the height ratio, Eckert number, viscosity ratio, and Prandtl number. At the bottom plate, the rate of heat transfer was enhanced with the height ratio, Eckert number and the Prandtl number, but decreased with the conductivity ratio, porous medium parameter, and viscosity ratio. The analysis presented here tallies with the classical Couette flow by choosing appropriate values for the governing parameters.

Acknowledgments The authors express their sincere thanks to all reviewers for their critical comments, valued suggestions, and also for their encouragement. One of the authors also thanks Prof. I. C. Liu, Department of Civil Engineering, National Chi Nan University, Puli, Nantou, Taiwan for his academic support.

Appendix

$$c_4 = \frac{\left(1-\frac{P}{2}\right)C\cosh(\sigma h) - \frac{Ph^2}{\lambda\sigma^2}(1 - C\cosh(\sigma h))}{S\sinh(\sigma h) + \lambda\sigma C\cosh(\sigma h)}; c_1 = \lambda\sigma c_4;$$

$$c_2 = 1 - \frac{P}{2} - c_1; c_3 = \frac{Ph^2}{\lambda\sigma^2} + c_2;$$

$$b_1 = -\frac{Ec\,\mathrm{Pr}\,P^2}{12}; b_2 = -\frac{Pc_1 Ec\,\mathrm{Pr}}{3}; b_3 = -\frac{Ec\,\mathrm{Pr}\,c_1^2}{2}; f_1 = -\frac{Ec\,\mathrm{Pr}\,\lambda\left(c_3^2 + c_4^2\right)}{4\lambda_T};$$

$$f_2 = -\frac{Ec\,\mathrm{Pr}\,\lambda c_3 c_4}{2\lambda_T}; f_3 = \frac{2Ec\,\mathrm{Pr}\,Ph^2 c_4}{\lambda_T\sigma^2}; f_4 = \frac{2Ec\,\mathrm{Pr}\,Ph^2 c_3}{\lambda_T\sigma^2}; f_5 = -\frac{Ec\,\mathrm{Pr}\,P^2 h^6}{2\lambda\lambda_T\sigma^2};$$

$$k_3 = \frac{h}{(\lambda_T + h)}\begin{pmatrix} -b_1 - b_2 - b_3 - \frac{\lambda_T}{h}\left(f_2\sigma h + f_3\sigma h\right) - f_1 - f_4 + 1 + f_1 C\cosh(2\sigma h) \\ -f_2 S\sinh(2\sigma h) - f_3 S\sinh(\sigma h) + f_4 C\cosh(\sigma h) + f_5 \end{pmatrix};$$

$$k_4 = k_3 - f_1 C\cosh(2\sigma h) + f_2 S\sinh(2\sigma h) + f_3 S\sinh(\sigma h) - f_4 C\cosh(\sigma h) - f_5;$$

$$k_2 = f_1 + f_4 + k_4; k_1 = 1 - k_2 - b_1 - b_2 - b_3.$$

References

Alazami, M., Vafai, K.: Analysis of fluid flow and heat transfer interfacial conditions between a porous medium and a porous layer. Int. J. Heat Mass Transfer **44**, 1735–1749 (2001)

Al-Nimr, M.A., Alkam, M.K: Unsteady non-Darcian fluid flow in parallel channels partially filled with porous material. Heat Mass Transfer **33**, 315–318 (1998)

Beavers, G.S., Joseph, D.D.: Boundary conditions at naturally permeable wall. J. Fluid Mech. **13**, 197–207 (1967)

Chikh, S., Boumedian, A., Bouhadef, K., Lauriat, G.: Analytical solution of non-Darcian forced convection in an annular duct partially filled with porous medium. Int. J. Heat Mass Transfer **38**, 1543–1551 (1995)

Giveler, R.C., Altobelli, S.A.: A determination of the effective viscosity for the Brinkman–Forchhiemer flow model. J. Fluid Mech. **258**, 355–370 (1994)

Kaviany, M.: Principle of Heat Transfer in Porous Media. 2nd edn. Springer, New York (1995)

Kuznetsov, A.V.: Analytical investigation of Couette flow in a composite channel partially filled with a porous medium and partially with a clear fluid. Int. J. Heat Mass Transfer **41**, 2556–2560 (1998)

Martys, N., Bentz, D.P., Garboczi, E.J.: Computer simulation study of the effective viscosity in Brinkman's equation. Phys. Fluids **6**, 1434–1439 (1994)

Nakayama, A., Kokudai, T., Koyama, H.: Non-Darcian boundary layer flow and forced convective heat transfer over a flat plate in a fluid-saturated porous medium. ASME J. Heat Transfer **112**, 157–162 (1990)

Neild, D.A.: The limitations of the Brikman–Forchheimer equation in modeling flow in a saturated porous medium and at an interface. Int. J. Heat Mass Transfer **12**, 269–272 (1991)
Nield, D.A., Bejan, A.: Convection in Porous Media. 2nd edn. Springer, New York (1999)
Ochoa-Tapia, J.A., Whitaker, S.: Momentum transfer at the boundary between a porous medium and a homogeneous fluid I: theoretical development. Int. J. Heat Mass Transfer **38**, 2635–2646 (1995)
Prasad, V.: Convection flow interaction and heat transfer between fluid and porous layers. In: Proceedings of NATO Advanced Study Institute on Convective Heat and Mass Transfer in Porous Media, Turkey (1990)
Prasad, V., Kulacki, F., Keyhani, M.: Natural convection in porous media. J. Fluid Mech. **150**, 89–119 (1985)
Rudraiah, N.: Forced convection in a parallel plate channel partially filled with a porous material. ASME J. Heat Transfer **107**, 331–332 (1985)
Umavathi, J.C, Chamkha, A.J., Mateen, A., Al-Mudhaf, A.: Oscillatory flow and heat transfer in a horizontal composite porous medium channel. Int. J. Heat Technol. **24**, 75–86 (2007)
Umavathi, J.C., Prathap Kumar, J., Malshetty, M.S.: Convective flow and heat transfer in composite porous medium. J. Porous Media **4**, 15–22 (2001)
Vafai, K., Kim, S.J.: Fluid mechanics of interface region between a porous medium and a fluid layer—an exact solution. Int. J. Heat Mass Transfer **11**, 254–256 (1990)
Vafai, K., Kim, S.J.: On the limitation of the Brinkman Forchheimer-extended Darcy equation. Int. J. Heat Mass Transfer **16**, 11–15 (1995)